

# Sum-modified-Laplacian-based Multifocus Image Fusion Method in Cycle Spinning Sharp Frequency Localized Contourlet Transform Domain

QU Xiao-bo<sup>1</sup> YAN Jing-wen<sup>2,1</sup> YANG Gui-de<sup>2</sup>

(1. Department of Communication Engineering, Xiamen University, Xiamen 361005, China)

(2. Key Lab of Digital Signal and Image Processing of Guangdong Province, Shantou University, Shantou 515063, China)

**Abstract:** Sum-modified-Laplacian-based multifocus image fusion algorithm in cycle spinning sharp frequency localized contourlet transform (SFLCT) domain is proposed in this paper. SFLCT successfully reduces significant amount of aliasing components of the original contourlet which are located far away from the desired support. However, downsamplers and upsamplers presented in directional filter banks of SFLCT make it not shift-invariant and easily cause pseudo-Gibbs phenomena around singularities. Thus, we apply cycle spinning to compensate for the lack of translation invariance property. Furthermore, typical measurements for multifocus image fusion in spatial domain are introduced into contourlet domain and Sum-modified-Laplacian (SML), evidenced in this paper with the best capability to distinguish coefficients is from the clear parts or blurry parts of images, is employed in SFCLT subbands as measurement to compose coefficients of fused images. Experimental results demonstrate the proposed fusion method outperforms block-based spatial SML method, typical cycle spinning wavelet and shift-invariant wavelet methods, and typical cycle spinning contourlet methods in term of visual appearance and objective criteria for multifocus images.

**Keywords:** Image fusion, contourlet, pseudo-Gibbs phenomena, wavelet

## 1 Introduction

Imaging cameras, particularly those with long focal lengths, usually have only a finite depth of field. It is often not possible to get an image that contains all relevant objects in focus. Images are clear with good-focus and blurry with out-of-focus. So, a good-focus image is important for the human perception and machine vision. Image fusion is a good way to obtain a focalized image by combining multiple sensors data and providing more reliable and accurate information [1] [2]. For multifocus image fusion, this information is from the clear parts of source with good-focus.

There are two main methods for multifocus image fusion. One is selecting pixels from clear parts in the spatial domain to compose fused images [3]-[4]. Most of these methods are combing the blocks according to a measurement which evaluate the part is clear or not. These blocks are often in form of window with certain size or regional parts obtained by segmenting images. However, window-based method may easily produce block effect which affects the appearance of fused image a lot. And segmentation-based method is strongly dependent on the segmentation algorithm which is also another difficult problem in image processing. More badly, if an object of one source image is partly clear and partly blurry, the blurry part may be selected as part of the fused image when considering the integrality of the segmented part.

Another multifocus fusion method is combing the coefficients in multiscale decomposition (MSD) transform domain under the assumption that image details are contained in the high-frequency subbands. These transforms could be wavelet [2], bandelet [5], curvelet [6] and contourlet [7]-[9]. One of the well-known MSD methods for image fusion is wavelet [2].

However, traditional separable wavelet can only capture limited directional information and will not see the smoothness along contours [10]. Contourlet [10] solves the two-dimensional or high dimensional discontinuities and offers a flexible multiresolution and directional decomposition for images. It has been successfully employed and evidenced to outperform wavelet in image processing [10] - [12] including image

fusion [7]-[9]. Unfortunately, the original contourlet [10] exhibit some fuzzy artifacts along the main image ridges because of non-ideal filter. Yue Lu [13] proposes a new construction of the contourlet, called sharp frequency localization contourlet transform (SFLCT) and alleviates the non-localization problem.

However, due to downsamplers and upsamplers presented in the directional filter banks of SFLCT, SFLCT is not shift-invariant, which easily causes pseudo-Gibbs phenomena around singularities and is important in multifocus image fusion[8][14][15]. In this paper, we apply cycle spinning [14][15] to compensate for the lack of translation invariance property of SFLCT, named as CS-SFLCT, and introduce it into image fusion.

In addition, a good fusion method not only on relies on the transform but also depend on how to combine the coefficients in transform domain. Particularly, for multifocus image fusion, the key point is establishing a good measurement to successfully distinguish the coefficients is from the clear parts from blurry parts. Thus, some typical measurements in the spatial domain [2] are compared and we introduce sum-modified-Laplacian (SML) of the coefficients as a measurement. Coefficients with greater SML are selected out to compose fused image when high-frequency subbands of source images are compared. We name the proposed fusion method as CS-SFLCT-SML in this paper.

The outline of this paper is as follows: Section 2 brief introduces CS-SFLCT and give framework of applying CS-SFLCT to image fusion. Section 3 proposes SML-based fusion rule basing on performance comparison of focus measurements. Section 3 gives the fruitful experiments to show the advantage of CS-SFLCT-SML on suppressing Gibbs-phenomena and selecting coefficients from clear parts. Then conclusion and discussion are given in section 5.

## 2 Cycle spinning Sharp Frequency Localized Contourlet Transform for Image Fusion

### 2.1 Sharp Frequency Localized Contourlet Transform

The original contourlet [10] is constructed by the combination of laplacian pyramid, which is first used

to capture the point discontinuities, and the directional filter banks (DFB), which is used to link point discontinuities into linear structure. In the frequency domain, the laplacian pyramid iteratively decompose a two dimensional image into lowpass and highpass subbands and the DFB divide the highpass subbands into directional subbands.

When non-ideal filters are combined with laplacian pyramid, the contourlets are not localized in frequency, with substantial amount of aliasing components outside of the desired trapezoid-shaped support [13]. To solve this problem, Yue Lu [13] proposes a new construction of a sharp frequency localization contourlet (SFLCT). Since the combination of laplacian pyramid and directional filters banks make the aliasing problem serious, new multiscale pyramid with different set of lowpass and highpass filters for the first level and all other levels are employed. Suppose lowpass filters  $L_i(\omega)(i=0,1)$  in the

frequency domain as  $L_i(\omega) = L_i^{1d}(\omega_1) \bullet L_i^{1d}(\omega_2)$

and  $L_i^{1d}(\omega)$  is a 1-D lowpass filter with passband

frequency  $\omega_{p,i}$  and stopband frequency  $\omega_{s,i}$  and a smooth transition band, defined as

$$L_i^{1d}(\omega) = \begin{cases} 1 & \text{for } |\omega| \leq \omega_{p,i} \\ \frac{1}{2} + \frac{1}{2} \cos \frac{(|\omega| - \omega_{p,i})\pi}{\omega_{s,i} - \omega_{p,i}} & \text{for } \omega_{p,i} < |\omega| < \omega_{s,i} \\ 0 & \text{for } \omega_{s,i} < |\omega| < \pi \end{cases}$$

for  $|\omega| \leq \pi$  and  $(i=0,1)$ .

Under the assumption that aliasing can be completely cancelled, the perfect reconstruction of multiscale pyramid should satisfy

$$|L_i(\omega)|^2 + |D_i(\omega)|^2 \equiv 1, \quad \text{for } i=0,1$$

Fig.1 shows the comparison on basis image of the original contourlet and SFLCT. (a) and (b) indicate that the frequency non-localization problem is serious in the original contourlet while this problem is suppressed by new contourlet construction and the spatial regularity of contourlet is greatly improved in SFLCT as shown in (c) and (d).

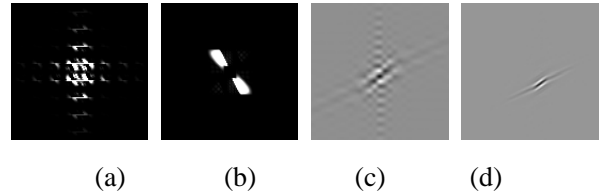


Fig.1 Basis images of original contourlet and sharp frequency localized contourlet (SFLCT). (a) and (b) are basis images of original contourlet and SFLCT in frequency domain, (c) and (d) are basis images of the two transforms in spatial domain.

## 2.2 Cycle Spinning Sharp Frequency Localized Contourlet Transform for Image Fusion

Unfortunately, downsamplers and upsamplers presented in the directional filter banks of SFLCT makes it lack shift-invariance, which could easily produce artifacts around the singularities, e.g. edges. Thus, Cycle Spinning (CS) [14] [15] is employed in this paper to compensate for the lack of translation invariance. It is a simple yet efficient way to improve the performance for a shift variant transform. For simplicity, we call the new form of SFLCT as CS-SFLCT.

Suppose  $f_1, f_2$  and  $F$  are the source and fused images,  $C$  and  $C_{-1}$  are the forward and inverse

SFLCT,  $S_{x,y}$  is the cycle spinning method and  $x, y$  are the shift arranges in horizontal and vertical directions, and  $h$  is the fusion process in SFLCT domain, the CS-SFLCT image fusion method could be described as follows and the framework is shown Fig.2.

$$F = S_{-x,-y} \left\{ h \left[ C \left( S_{x,y} (f_1) \right), C \left( S_{x,y} (f_2) \right) \right] \right\}$$

Usually,  $x \in X$  and  $y \in Y$  indicate a series of shift arranges  $X = \{x_1, x_2, \dots, x_m\}$  and

$Y = \{y_1, y_2, \dots, y_n\}$ . If the size of source images are  $M \times N$ , the maximum shift  $x_{\max} = \max(X)$  in

horizontal direction must satisfy  $x_{\max} \leq M$  and the

maximum shift  $y_{\max} = \max(Y)$  in vertical direction

must satisfy  $y_{\max} \leq N$ . Therefore, Cycle spinning averages out the translation dependence of subsampled directional filter banks as

$$F = Ave_{x \in X, y \in Y} \left\{ S_{-x, -y} \left\{ h \left[ C(S_{x \in X, y \in Y}(f_1)), C(S_{x \in X, y \in Y}(f_2)) \right] \right\} \right\}$$

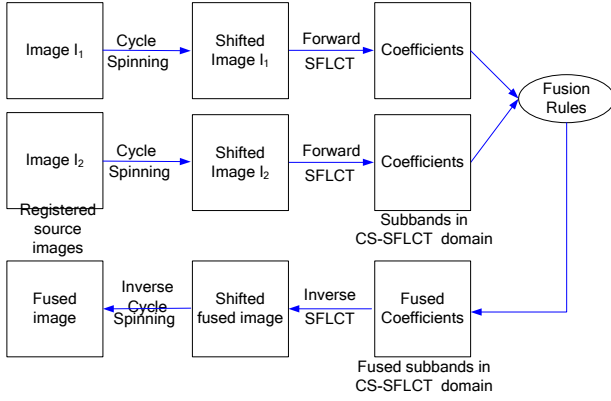


Fig.2 Framework of Image Fusion Method using Cycle Spinning Sharp Frequency Contourlet Transform.

### 3 Fusion Rules

For image fusion, how to combine the coefficients in MSD domain is another key point. Generally, coefficients with high activity-level, typically with maximum absolute values, are selected to compose the fused image [2]. Particularly, for multifocus image fusion, coefficients which are with high variation and from the clear parts of source images are selected to compose the fused image.

#### 3.1 Fusion of low-frequency coefficients

Considering approximate information of image is constructed by the low-frequency coefficients [2], average rule is adopted for low-frequency coefficients. Suppose  $B_F^{l,k}(i, j)$  is the fused low-frequency coefficients located at  $(i, j)$  in the  $l$ -th scale and  $k$ -th direction subband, then

$$B_F^{l,k}(i, j) = \frac{B_1^{l,k}(i, j) + B_2^{l,k}(i, j)}{2} \quad (1)$$

where  $B_1^{l,k}(i, j)$  and  $B_2^{l,k}(i, j)$  denote the low-frequency coefficients located at the same place of subbands.

#### 3.2 Fusion of high-frequency coefficients

Under the assumption that image details are contained in the high-frequency subbands in MSD

transform domain, the typical fusion rule is maximum-based rule, which selects high-frequency coefficients with maximum absolute value [2], named as Coeffs-max rule in this paper.

For multifocus image fusion, many typical focus measurements, e.g. energy of image gradient (EOG), Tenengrad, spatial frequency (SF) and laplacian energy (EOL) and SML in the spatial domain are compared in [3]. They all measure the variation of pixels. Pixels with greater values of these measurements, when source images are compared, are considered from clear parts and selected as the pixels of the fused image. Since subbands of multifocus images in SFLCT domain can be viewed as image and the variation of subbands also exist as shown in the labeled region of Fig.3 (d) and (e), therefore it is reasonable to utilize EOG, Tenengrad, SF, EOL and SML as the measurements to select coefficients from the clear parts of source images.

However, to be different from the measurements defined in [3], coefficients in the SFLCT domain, not the pixel value in spatial domain, are used to compute the measurements. For example, suppose  $I^{l,k}(i, j)$  denotes the coefficient located at  $(i, j)$  in the  $l$ -th scale and  $k$ -th direction subband, the modified Laplacian (ML) and SML is defined as follows:

$$ML^{l,k}(i, j) = \left| 2I^{l,k}(i, j) - I^{l,k}(i - \text{step}, j) - I^{l,k}(i + \text{step}, j) \right| + \left| 2I^{l,k}(i, j) - I^{l,k}(i, j - \text{step}) - I^{l,k}(i, j + \text{step}) \right|$$

where  $step$  is a variable spacing between coefficients and in this paper  $step$  always equals 1.

$$SML^{l,k}(i, j) = \sum_{p=-P}^P \sum_{q=-Q}^Q \left[ ML^{l,k}(i + p, j + q) \right]^2 \quad (2)$$

where the parameters  $P$  and  $Q$  determine the window with size  $(2P+1) \times (2Q+1)$  are used to compute the measurement.

Now, the problem is the capability of these measurements to distinguish coefficients may be different from the conclusion in [2] because we employ measurements in SFLCT domain. Thus, we use root mean square error (RMSE) to evaluate the performance of focus measurements when we know the focalized and clear image, also called reference image.

RMSE is defined as

$$RMSE = \sqrt{\frac{\sum_{i=1}^M \sum_{j=1}^N (R(i,j) - F(i,j))^2}{M \times N}} \quad (3)$$

where  $R$  and  $F$  are reference image and fused image respectively, with size  $M \times N$  pixels.

In order to compare these measurements equally, they are evaluated in form of window with save size, which means measurement of neighboring coefficients are summed up. In this experiment, Fig.3 (a) are (b) are source images with size  $256 \times 256$ , and Fig.3(c) is the reference image. RMSE performances of these measurements are compared in Tab.1. It shows that RMSE of SML-based fusion method is the lowest one, which means using SML as the measurement in the SFLCT domain could produces best fused result for multifocus image fusion. In our other experiments, we get the same results and do not present them here due to the limit of paper length. Thus, not only SML is proved to be the best measurement in spatial domain [3], but also SML is very efficient in the SFLCT domain. Therefore, it is reasonable to use SML to select the coefficients in the SFLCT domain.

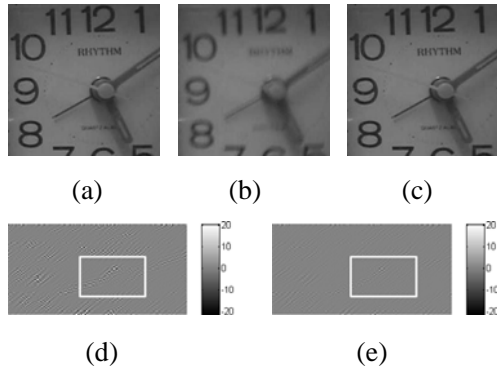


Fig.3 Multifocus source images and high-frequency subbands.(a)reference image, (b) blurry source image,(c) good-focus source image, (d) and (e) are the one of the high-frequency subbands of (b) and (c) with the same direction and scale in the SFLCT domain, respectively.

Tab.1 RMSE Performance of different measurements

Measurement	EOG	EOL	Tenengrad	SF	SML
RMSE	2.0391	2.0233	2.0977	2.0686	1.9502

Suppose  $I^{l,k}(i,j)$  and  $I_F^{l,k}(i,j)$  denote the coefficient of source and fused images according to the same location while  $SML_1^{l,k}(i,j)$  and  $SML_2^{l,k}(i,j)$  denote the SML measurement of  $I^{l,k}(i,j)$  and  $I_F^{l,k}(i,j)$ , respectively, the proposed SML-based fusion rule can be described as follows:

$$I_F^{l,k}(i,j) = \begin{cases} I_1^{l,k}(i,j), & \text{if } SML_1^{l,k}(i,j) \geq SML_2^{l,k}(i,j) \\ I_2^{l,k}(i,j), & \text{if } SML_1^{l,k}(i,j) < SML_2^{l,k}(i,j) \end{cases} \quad (4)$$

It means coefficients with maximum SML measurement are selected as the coefficients of the fused image when subbands are compared in the CS-SFLCT domain. We name this fusion rule as SML-max rule and name the proposed fusion method as CS-SFLCT-SML for simplicity.

## 4 Experimental Results

In this section, CS-SFLCT-SML algorithm is utilized to combine multi-focus images. Decomposition parameter of contourlet, SFLCT and CS-SFLCT are all set as [2,3,3,4,4] in the DFB stage decomposition. In the following experiments, four pairs of multifocus images are used as the source images shown in Fig.4.

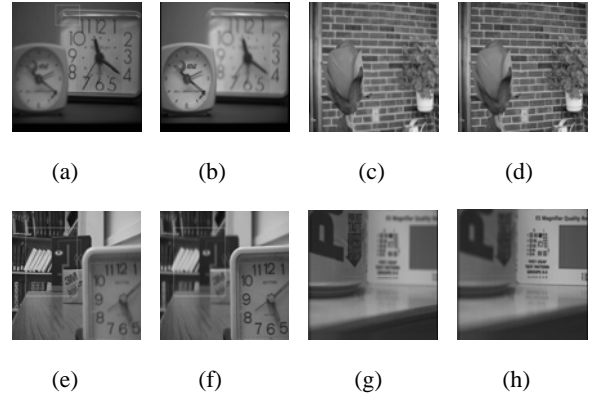


Fig.4 Source images for multifocus fusion. (a) and (b),(c) and (d),(e) and (f),(g) and (h), are the pairs, which are partly defocused and partly in good-focus.

In order to show the advantages of the new method, we establish four steps to demonstrate that the proposed CS-SFLCT-SML outperforms other fusion methods. First, CS-SFLCT is compared with original contourlet (OCT), cycle spinning original contourlet (CS-OCT) and SFLCT to show the advantage of suppressing pseudo-Gibbs phenomena around singularities. Second, the influence of shift arranges on fusion performance are analyzed. Third, SML-max rule is compared with Coeffs-max rule. Finally, CS-SFLCT-SML is compared with other typical fusion methods based on block-based spatial SML method [3], shift-invariant wavelet method using Coeffs-max rule (SIWT-max) [2] [16], cycle spinning wavelet method [16] [17] using maximum rule (CS-WT-max).

In experiments, besides visual appearance

observation, mutual information (MI) [18] and  $Q^{AB/F}$  [19] are employed as information-based objective criteria. The reason is that image fusion aims at combining information and these criteria do not require the information of ideal fused image. MI essentially computes how much information from source images is transferred to the fused image, while  $Q^{AB/F}$  measures the amount of edge information transferred from the source images to the fused images using a Sobel edge detector.

#### 4.1 Suppress pseudo-Gibbs phenomena using CS-SFLCT

In this section, the original contourlet and SFLCT, which both lack shift-invariance and easily result in pseudo-Gibbs phenomena around singularities, e.g. edges, are compared with CS-OCT[8][14] and CS-SFLCT proposed in this paper, which both employ the cycle spinning to overcome the pseudo-Gibbs phenomena, in image fusion. Shift arranges of CS-OCT and CS-SFLCT is set as  $X=Y= \{-1,-2,-4,-8,1,2,4,8\}$ . In transform domain, typical average and Coeffs-max rules are adopted in the low-frequency and high-frequency subbands.

Tab. 2 shows the comparison on objective criteria using different forms of contourlet for image fusion. It indicates CS-OCT obtains greater MI and  $Q^{AB/F}$  than OCT while CS-SFLCT obtains greater MI and  $Q^{AB/F}$  than SFLCT. The objective criteria of CS-SFLCT are the greatest among the four forms of contourlet. So, cycle spinning could lead contourlet transforms to transfer more information to the fused image and CS-SFLCT performs best.

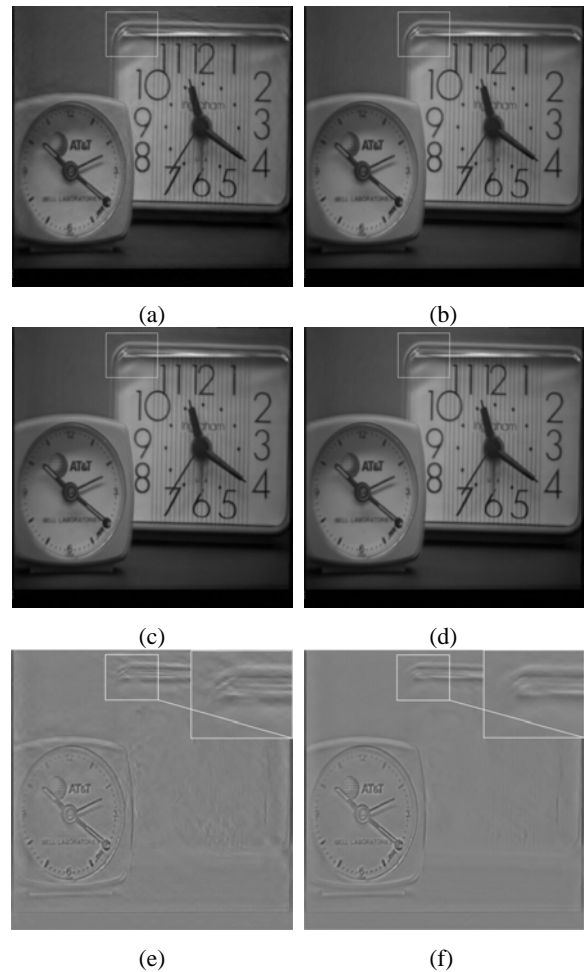
Fig.5 depicts the visual appearance of fused images shown in Fig.4 (a) and Fig.4 (b). Because source image Fig.4 (a) is clear in the labeled part, so the lower residue features in the difference images, which are gotten by subtracting Fig.4 (a), means the better the contourlet transfer features of source images to fused images. Especially, blurry edges, presented in the zoomed out parts, show the pseudo-Gibbs phenomena which reduces visual quality of the fused images. One can see blurry edges of CS-OCT are less than those of OCT while CS-SFLCT obtains less blurry edges than SFLCT. Thus, cycle spinning is a good way to compensate pseudo-Gibbs phenomena when

shift-variant contourlet are used. This conclusion is consistent with objective criteria shown in Tab. 2.

Further more, the greatest values of MI and  $Q^{AB/F}$  and the least blurry edges presented in the zoomed out part of difference image in Fig.5 (h) demonstrate that CS-SFLCT is the best contourlet transform for image fusion among the four forms discussed in this section.

Tab 2. Comparison on objective criteria using different forms of contourlet in image fusion.

Images	Criteria	OCT	CS-OCT	SFLCT	CS-SFLCT
Fig.4 (a) and (b)	MI	5.9159	6.4528	6.4590	6.5545
	$Q^{AB/F}$	0.6079	0.6532	0.6552	0.6628
Fig.4 (c) and (d)	MI	4.8757	5.3899	5.4064	5.4849
	$Q^{AB/F}$	0.6443	0.6851	0.6888	0.6953
Fig.4 (e) and (f)	MI	5.1597	5.7224	5.7429	5.8703
	$Q^{AB/F}$	0.6131	0.6598	0.6635	0.6734
Fig.4 (g) and (h)	MI	6.1247	6.5997	6.5550	6.6752
	$Q^{AB/F}$	0.7111	0.7571	0.7507	0.7581



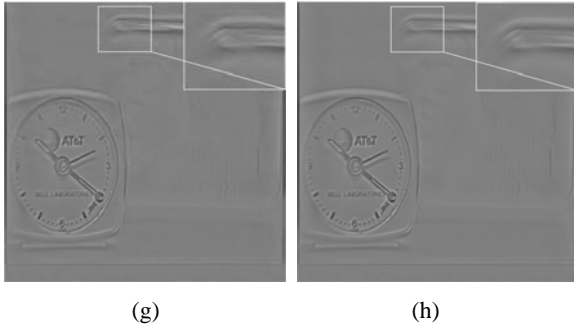
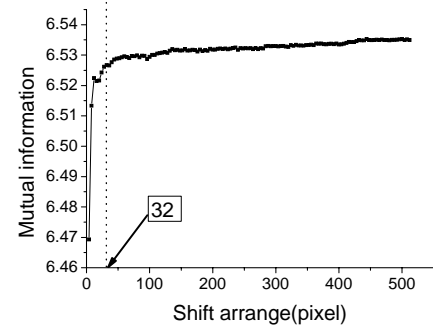


Fig. 5 Suppress the pseudo-Gibbs phenomena using cycle spinning. (a), (b), (c) and (d) are fused results using OCT, CS-OCT, SFLCT and CS-SFLCT respectively. (e), (f), (g) and (h) are the difference image which (a), (b), (c) and (d) minus the source image shown in Fig.4 (a).

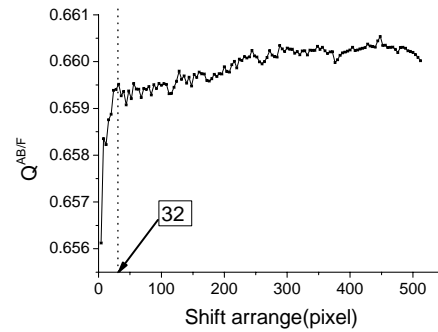
#### 4.2 The influence of shift arranges on fusion performance

Since the shift arrange would affect the performance on remedy pseudo-Gibbs phenomena, we will test objective criteria performance versus different shift arranges in this section. Fig.4 (a) and (b) are fused as the example here. We set  $X = Y = \{4, 8, 12, \dots, x_{\max}\}$  and the maximum shift arranges is changed from 4-pixels to 512-pixels distance with  $x_{\max} = 4i$ ,  $i = 1, 2, 3, \dots, 128$ .

Objective criteria shown in Fig.6 indicate that MI and  $Q^{AB/F}$  increases quickly when maximum shift arrange  $x_{\max}$  is small. However, objective criteria nearly do not improve when  $x_{\max}$  reaches a certain constant, for example  $x_{\max} = 32$  in this experiments for fusing Fig.4 (a) and (b) with  $512 \times 512$  size. Though  $Q^{AB/F}$  curve changes slightly when  $x_{\max}$  is larger than 32, but the value of  $Q^{AB/F}$  only changes from 0.6595 to 0.6605. So, we only need  $\frac{32}{4} = 8$  times shift on X and Y dimensions to suppress the pseudo-Gibbs phenomena very well. Thus, cycle spinning is an efficient and simple way for image fusion to overcome the shift-variance of SFLCT.



(a)



(b)

Fig.6 Objective criteria versus shift arrange using CS-SFLCT in image fusion. (a) mutual information curve, (b)  $Q^{AB/F}$  curve.

#### 4.3 SML-based Fusion Rule in CS-SFLCT domain

In this section, we will show why SML-based fusion rule could improve the fusion performance. SML-max rule and Coeffs-max rule are compared on high-frequency subbands in the CS-SFLCT domain with shift arranges  $X=Y = \{-1, -2, -4, -8, 1, 2, 4, 8\}$ . We take labeled parts of Fig.4 (e) and (f), as the example to easily understand why SML-max rule could improve the fusion performance.

Fig.7 (a) and (b) shows the high-frequency subbands in CS-SFLCT domain. One can see that values of coefficients in the clear part are greater than those of blurry part. That is why typical Coeffs-max is used in MSD-based fusion methods.

Fig.7 (c) and (f) shows the decision maps in which the white color indicates coefficients are selected from Fig.7 (a), otherwise selected from Fig.7 (b). Since labeled part of Fig.4 (e) is clearer than that of Fig.4 (f), the optimal decision map would be in white color in the whole decision map, which means all coefficients should be selected from Fig.7 (a), which is a high subband of Fig.4 (e).

However, decision map of Coeffs-max rule, shown in

Fig.7 (c), indicates that this rule does not select the coefficients from the clear part completely. And if we evaluate the high-frequency subbands with SML, considering regional information and gradient energy, more coefficients are selected out from clear source image. The decision map is shown in Fig.7 (f). As a result, fused image is more like the good-focus source images using SML-max rule, rather than using Coeffs-max rule. This conclusion is also evidenced in Tab.3 which shows SML-max rule obtains greater objective criteria than Coeffs-max rule.

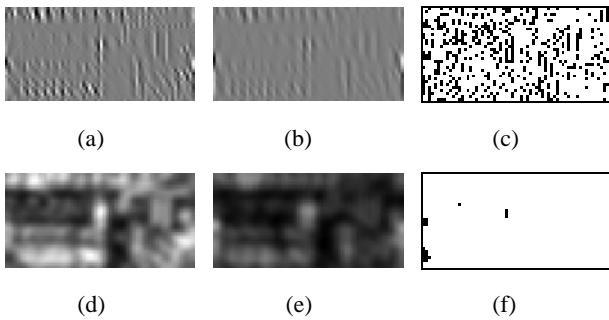


Fig.7 Comparisons on SML-max and Coeffs-max rules. (a) and (b) are one high-frequency subbands of the labeled part in Fig.4(e) and Fig.4 (f), (d) and (e) are SML values of (a) and (b), (c) and (f) are decision maps of SML-max and Coeffs-max rules, respectively.

Tab.3 Comparison on objective criteria using SML-max and Coeffs-max rules in image fusion.

Images	Criteria	Coeffs-max	SML-max
Fig.4 (a) and (b)	MI	6.5545	6.7401
	$Q^{AB/F}$	0.6628	0.6754
Fig.4 (c) and (d)	MI	5.4849	5.5468
	$Q^{AB/F}$	0.6953	0.7051
Fig.4 (e) and (f)	MI	5.8703	6.1716
	$Q^{AB/F}$	0.6734	0.6992
Fig.4 (g) and (h)	MI	6.6752	6.8646
	$Q^{AB/F}$	0.7581	0.7727

#### 4.4 Comparisons on typical fusion methods

In this section, block-based spatial SML methods with  $8 \times 8$  blocks(BBS-SML)[3], shift-invariant wavelet using maximum rule(SIWT-max)[2][16], cycle spinning form of wavelet using maximum rule(CS-WT-max) [16][17] and the proposed method CS-SFLCT-SML are compared. In CS-DWT-max and CS-SFLCT-SML, shift arrange is set as  $X=Y=\{-1,-2,-4,-8,1,2,4,8\}$  and decomposition level is 5. In order to show the influence on the fused image, no

majority filter is used for selecting pixels or coefficients.

Fig.8 shows the fused results using typical fusion methods. Obviously, fused image of BBS-SML presents block effect. Though BBS-SML obtains greatest objective criteria shown in Table 4, block effect is fatal and reduce the image quality for image fusion because image fusion serves for human and machine perceptions. Though one may use majority filter as the remedy to improve the performance, block effects could only be suppressed to a certain degree but not completely, particularly when pixels of block are partly clear and partly blurry. MSD transform can successfully overcome this disadvantage because coefficients in subbands, not pixels in spatial domain, are considered as image details and selected out to compose fused images. This is why many researchers would like to use MSD in image fusion. In addition, SIWT-max and CS-WT-max methods result in blurry around edges, especially in the labeled parts shown in Fig.8 (b) and (c). And the proposed CS-SFLCT-SML presents the best visual appearance.

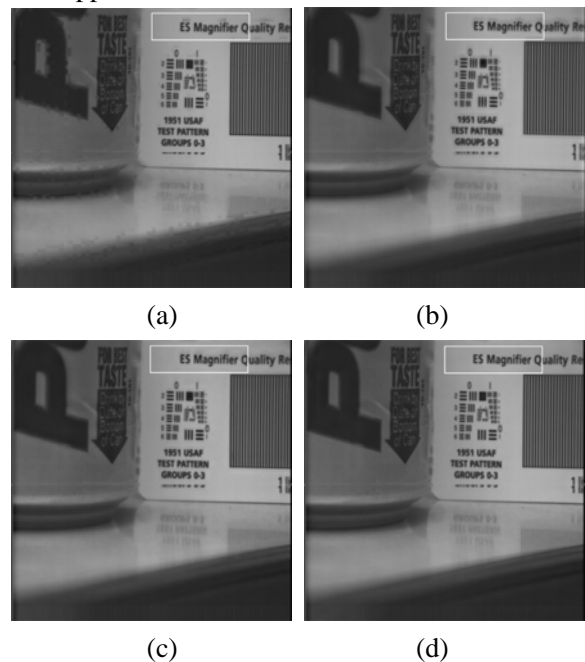


Fig.8 Comparison on visual appearance using different typical fusion methods. (a)-(d) are the fused image using block-based spatial SML methods, shift-invariant wavelet, cycle spinning wavelet and the proposed CS-SFLCT-SML methods, respectively.

Tab.4 Comparison on objective criteria using typical fusion methods.

Images	Criteria	BBS-SML	SIWT-max	CS-WT-max	CS-SFLCT-SML
Fig.4 (a) and (b)	MI $Q^{AB/F}$	8.7882 0.7216	6.4409 0.6829	6.4195 0.6595	6.7401 0.6754
Fig.4 (c) and (d)	MI $Q^{AB/F}$	8.1046 0.7243	4.9494 0.7098	5.2684 0.6921	5.5468 0.7051
Fig.4 (e) and (f)	MI $Q^{AB/F}$	8.0882 0.7332	5.7311 0.6752	5.7124 0.6702	6.1716 0.6992
Fig.4 (g) and (h)	MI $Q^{AB/F}$	8.3287 0.7695	6.3964 0.7464	6.5282 0.7563	6.8646 0.7727

## 4 Conclusion

In this paper, a sharp frequency localization contourlet transform (SFLCT) is introduced to image fusion and cycle spinning (CS) is adopted to improve performance on suppressing the pseudo-Gibbs phenomena in image fusion. Furthermore, for multifocus images, typical measurements in the spatial domain are introduced into contourlet domain and their capabilities to distinguish coefficients from clear or blurry parts of images are compared. Sum-modified-Laplacian (SML) is evidenced as the best measurement thus we propose the SML-based fusion rule in SFLCT domain. Experimental results demonstrate that the proposed CS-SFLCT-SML fusion method outperforms block-based spatial SML method, typical cycle spinning wavelet and shift-invariant wavelet methods, and typical cycle spinning contourlet methods.

## References

- [1] D L Hall, J Llinas. An introduction to multi-sensor data fusion[J]. Proc. of the IEEE, 1997, 85(1): 6-23.
- [2] Z. Zhang and R. S. Blum. A categorization of multiscale-decomposition-based image fusion schemes with a performance study for a digital camera application [J], Proc. of the IEEE, 1999, 87(8):1315-1326.
- [3] Wei Huang, Zhongliang Jing. Evaluation of focus measures in multi-focus image fusion [J], Pattern Recognition Letters, 2007, 28(4): 493-500.
- [4] Shutao Li, Bin Yang. Multifocus image fusion using region segmentation and spatial frequency[J], Image and Vision Computing, 2008, 26(7): 971-979.
- [5] Xiaobo Qu, Jingwen Yan, Guofu Xie, et al. A novel image fusion algorithm based on bandelet transform [J], Chinese Optics Letters, 2007, 5(10):569-572.
- [6] Zhang Qiang, Guo Bao-long. Fusion of remote sensing images based on the second generation Curvelet transform [J], Optics and Precision Engineering, 2007, 15(7):1130-1136.(in Chinese)
- [7] Miao Qiguang, Wang Baoshu. A novel image fusion method using contourlet transform [A]. Proc. 2006 International Conference on Communications, Circuits and Systems Processing[C], 2006, 548-552.
- [8] Liang Dong, Li Yao, Shen Min, et al. An Algorithm for Multi-Focus Image Fusion Using Wavelet Based Contourlet Transform [J], Acta Electronica Sinica ,2007,35(2):320-322 (in Chinese)
- [9] Li Guang-xin,Wang Ke. Color image fusion algorithm using the contourlet transform[J], Acta Electronica Sinica ,2007, 35(1):112-117 (in Chinese)
- [10] M N Do and M Vetterli. The contourlet transform: an efficient directional multiresolution image representation[J], IEEE Trans. Image Proc. 2005,14(12):2091-2106.
- [11] Jiao Licheng,Tan Shan. Development and Prospect of Image Multiscale Geometric Analysis[J], Acta Electronica Sinica, 2007,31(12A):1975-1981 (in Chinese)
- [12] Yan Jingwen, QU Xiaobo. Beyond Wavelets and Its Applications [M].Beijing: National Defense Industry Press, June 2008. (In Chinese)
- [13] Yue Lu, MN Do. A New Contourlet Transform with Sharp Frequency Localization [A], Proc. of 2006 IEEE International Conference on Image Processing[C], IEEE, Atlanta, USA, 2006, 1629-1632.
- [14] Eslami R, Radha H. The contourlet transform for image denoising using cycle spinning [A], Proc. of Asilomar Conference on Signals ,Systems, and Computers[C], 2003,1982-1986.
- [15] R. R. Coifman ,D. L. Donoho. Translation invariant de-noising, Wavelets and Statistics[M], Eds. New York: Springer-Verlag, A. Antoniadis and G. Oppenheim, 1995, 125-150.
- [16] Rockinger O, Fechner T.Pixel-level image fusion: The case of image sequences[A], Proc. SPIE[C], 1998,3374:378-388.
- [17] Oliver rockinger. Image Fusion Toolbox [EB/OL] <http://www.metapix.de/toolbox.htm>.
- [18] Guihong Qu, Dali Zhang, Pingfan Yan. Information measure for performance of image fusion[J]. Electronics Letters, 2002, 38 (7): 313-15.
- [19] V. Petrovic, C. Xydeas. On the effects of sensor noise in

---

pixel-level image fusion performance [A], Proc. of the  
Third International Conference on Image Fusion[C], IEEE  
Press, 2000, 2:14-19.